PROCEEDINGS OF SCIENCE

Charged particle multiplicities in inelastic pp events with the ATLAS detector

Alison LISTER[*†]
University of Geneva
E-mail: alison.lister@cern.ch

Measurements are presented from proton-proton collisions at centre-of-mass energies of $\sqrt{s} =$ 0.9, 2.36 and 7 TeV recorded with the ATLAS detector at the LHC. Events were collected using a single-arm minimum-bias trigger. The charged-particle multiplicity, its dependence on transverse momentum and pseudorapidity and the relationship between the mean transverse momentum and charged-particle multiplicity are measured. Measurements in different regions of phase-space are shown, providing diffraction-reduced measurements as well as more inclusive ones. The observed distributions are corrected to well-defined phase-space regions, using model-independent corrections. The results are compared to each other and to various Monte Carlo models, including a new AMBT1 PYTHIA6 tune. In all the kinematic regions considered, the particle multiplicities are higher than predicted by the Monte Carlo models.

35th International Conference of High Energy Physics - ICHEP2010,
July 22-28, 2010
Paris France

[*]Speaker.
[†]On behalf of the ATLAS Collaboration

PoS(ICHEP 2010)346

1. Introduction

Measurements of inclusive charged-particle distributions provide insight into the strong interactions at low energy-scales. Several QCD-inspired models have been developed to interpret them. These models are frequently cast into Monte Carlo simulations with free parameters that can be constrained by measurements such as minimum bias distributions. The results presented in these proceedings are inclusive-inelastic distributions, with minimal model-dependence; a minimum number of charged particles within well-defined transverse momentum, p_{T}, and pseudorapidity, η, selection are required.

The following distributions are measured:

$$\frac{1}{N_{\mathrm{ev}}}\cdot\frac{\mathrm{d}N_{\mathrm{ch}}}{\mathrm{d}\eta},\quad \frac{1}{N_{\mathrm{ev}}}\cdot\frac{1}{2\pi p_{\mathrm{T}}}\cdot\frac{\mathrm{d}^2N_{\mathrm{ch}}}{\mathrm{d}\eta\,\mathrm{d}p_{\mathrm{T}}},\quad \frac{1}{N_{\mathrm{ev}}}\cdot\frac{\mathrm{d}N_{\mathrm{ev}}}{\mathrm{d}n_{\mathrm{ch}}}\quad\text{and}\quad \langle p_{\mathrm{T}}\rangle \text{ vs. } n_{\mathrm{ch}},$$

where p_{T} is the charged particle momentum component transverse to the beam direction, η is the pseudorapidity of the particle, n_{ch} is the number of charged particles in an event, N_{ev} is the number of events with a minimum number of charged particles within the selected kinematic range, N_{ch} is the total number of charged particles in the data sample and $\langle p_{\mathrm{T}}\rangle$ is the average p_{T} for a given number of charged particles.

The charged-particle multiplicity results are compared to particle level Monte Carlo (MC) predictions. Three different phase-space regions are considered, with varying selection both on the p_{T} and the number of charged particles per event; all phase-space regions require tracks within $|\eta|<2.5$. Diffractive physics is expected to contribute mostly at low numbers of charged particles and at low track transverse momentum. Therefore varying the selection on n_{ch} and p_{T} in effect varies the relative contribution from diffractive events.

The reader is referred to the publication [1] for further details and the full results.

2. Data Samples, Monte Carlo Simulation

The ATLAS detector at the Large Hadron Collider (LHC) is described elsewhere [2]. For the measurements presented in these proceedings, the tracking devices and the trigger system are of particular importance.

These measurements use the first $\sim$190 $\mu\mathrm{b}^{-1}$ of data recorded by the ATLAS experiment at 7 TeV and $\sim$7 $\mu\mathrm{b}^{-1}$ at 0.9 TeV. Results are also presented at $\sqrt{s}=2.36$ TeV where the track reconstruction setup differs significantly from that at the other energies, due to the Silicon Tracker (SCT) not being at nominal voltage. The integrated luminosity at this energy is estimated to be $\sim$0.1 $\mu\mathrm{b}^{-1}$. Data were collected using a single-arm trigger overlapping with the acceptance of the tracking volume.

Inclusive minimum bias data are modeled using three components in the PYTHIA6 [3] Monte Carlo (MC) event generator: single-diffractive (SD), double-diffractive (DD) and non-diffractive (ND) processes. The samples used to determine detector acceptances and efficiencies and to correct the data are generated with the ATLAS MC09 PYTHIA tune [4].

Other particle level Monte Carlo samples are used to compare to corrected data (see paper [1] for full references): the new ATLAS Minimum Bias Tune 1 (AMBT1) PYTHIA6 tune, the DW PYTHIA6 tune, the PYTHIA8 generator, and the PHOJET generator.

3. Event Selection

Events in which the Inner Detector was fully operational and the solenoid magnet was on are used; at $\sqrt{s} = 2.36$ TeV the SCT was in standby due to there being no stable beams declared. Events were selected from colliding proton bunches in which the Minimum Bias Trigger Scintillator (MBTS) trigger recorded one or more counters above threshold on either side.

Three separate phase-space regions are considered with varying contributions from diffractive events: ≥ 1 charged particle in the kinematic range $p_{\mathrm{T}} > 500$ MeV, ≥ 6 charged particle in the kinematic range $p_{\mathrm{T}} > 500$ MeV, and ≥ 2 charged particles with $p_{\mathrm{T}} > 100$ MeV. All three regions consider particles with $|\eta| < 2.5$. These phase-space regions were chosen as they contain varying fractions of diffractive events.

In addition to the trigger selection and the phase-space region selection, to reduce the contribution from background events and non-primary tracks, as well as to minimise the systematic uncertainties, the events are required to satisfy the following criteria: the presence of a primary vertex reconstructed using the beam spot information and at least two tracks with similar properties to those used in the analysis; the rejection of events with a second vertex containing four or more tracks, to remove events with more than one interaction per bunch crossing; a minimum of one or two good tracks, depending on the particular phase-space region.

Good tracks are defined differently for the data at $\sqrt{s} = 7$ TeV and $\sqrt{s} = 0.9$ TeV than for those at $\sqrt{s} = 2.36$ TeV due to the SCT not being fully depleted for the runs at $\sqrt{s} = 2.36$ TeV. The tracks are defined [1] with relatively tight requirements on the number of hits in the detector and on the impact parameters with respect to the primary vertex.

4. Efficiency Corrections and Unfolding

The observed raw track distributions are corrected for a number of effects: event backgrounds, the trigger efficiency, the vertex reconstruction efficiency, the track reconstruction efficiency.

The effect of events lost due to the trigger and vertex requirements is corrected using an event-by-event weight. The p_{T} and η distributions of selected tracks are then corrected for the track reconstruction efficiency, for secondary contaminations and for tracks leaving the phase-space region of interest using a track-by-track weight.

For the particle multiplicity (n_{ch}) distribution, first, the observed track multiplicity distribution is corrected for the trigger and vertex reconstruction efficiencies. Then, an event-level correction is applied using an iterative Bayesian unfolding technique [5] to correct the observed track multiplicity to the distribution of the number of primary charged particles. This unfolding does not change the total number of events and thus an additional correction is applied to account for the events that were not present in our data sample due to the detector-level kinematic cuts.

The p_{T} distribution is also corrected using a similar unfolding method as used for the n_{ch} distribution.

The final particle level distribution of interest, $\langle p_{\mathrm{T}} \rangle$ versus n_{ch}, is obtained by correcting separately two components: the sum over the p_{T} of all the tracks in a given n_{ch} bin and the total number of tracks in that bin. The two distributions are first corrected on a track-by-track basis by applying the appropriate track weight, then the matrix obtained after the final iteration of the n_{ch} unfolding

procedure is applied, and finally the ratio of the two distributions is taken to obtain the corrected $\langle p_{\mathrm{T}} \rangle$ vs n_{ch} distribution.

The systematic uncertainties on each of the event-level and track-level efficiency corrections as well as those due to the unfolding techniques are computed separately with the effects on the final distribution added in quadrature. One of the dominant uncertainties is due to the track reconstruction efficiency, in particular the material uncertainty and the uncertainty due to the large extrapolation distances at high-η between the Pixel and the SCT detectors. The track reconstruction efficiency uncertainty tends to decrease with increasing p_{T} and increase with increasing $|\eta|$. Another dominant systematic uncertainty in the n_{ch} distribution is due to the fact that we only carry out unfolding in one variable at a time and thus the unfolding method for n_{ch} relies somewhat on the p_{T} spectrum of the particles in each bin. A method to re-weight the average p_{T} of tracks within a given n_{ch} bin is devised to obtain a systematic due to this effect.

5. Results

Figure 1 shows the four distributions measured in this analysis for the most inclusive phase-space region, $n_{\mathrm{ch}} \geq 2$, $p_{\mathrm{T}} > 100$ MeV at $\sqrt{s} = 7$ TeV. The data are compared to a variety of different MC models. Differences in the average charged particle multiplicity are visible in the η distribution while the p_{T} distribution shows deviations both at high and low p_{T}. The observed charged particle multiplicity is significantly higher than predicted for high multiplicities. The $\langle p_{\mathrm{T}} \rangle$ vs n_{ch} distribution shows how varied the models are even for distributions dominated by the tuning of only a few parameters of the MC.

Figure 2 shows the central mean charged particle density for all measurements in the three phase-space regions at three separate centre-of-mass energies. This shows the wide variety of predictions and energy extrapolations of the different MC tunes.

References

[1] ATLAS Collaboration, G. Aad *et al.*, Charged-particle multiplicities in pp interactions measured with the ATLAS detector at the LHC, Submitted to New J. Phys., arXiv:1012.5104 [hep-ex].

[2] ATLAS Collaboration, G. Aad *et al.*, The ATLAS Experiment at the CERN Large Hadron Collider, JINST **3** (2008) S08003.

[3] T. Sjöstrand, S. Mrenna, and P. Skands, PYTHIA 6.4 Physics and Manual, JHEP **05** (2006) 026, arXiv:hep-ph/0603175. version 6.4.21.

[4] ATLAS Collaboration, ATLAS Monte Carlo Tunes for MC09, ATL-PHYS-PUB-2010-002.

[5] G. D'Agostini, A Multidimensional unfolding method based on Bayes' theorem, Nucl. Instr. Meth. **A362** (1995) 487-498.

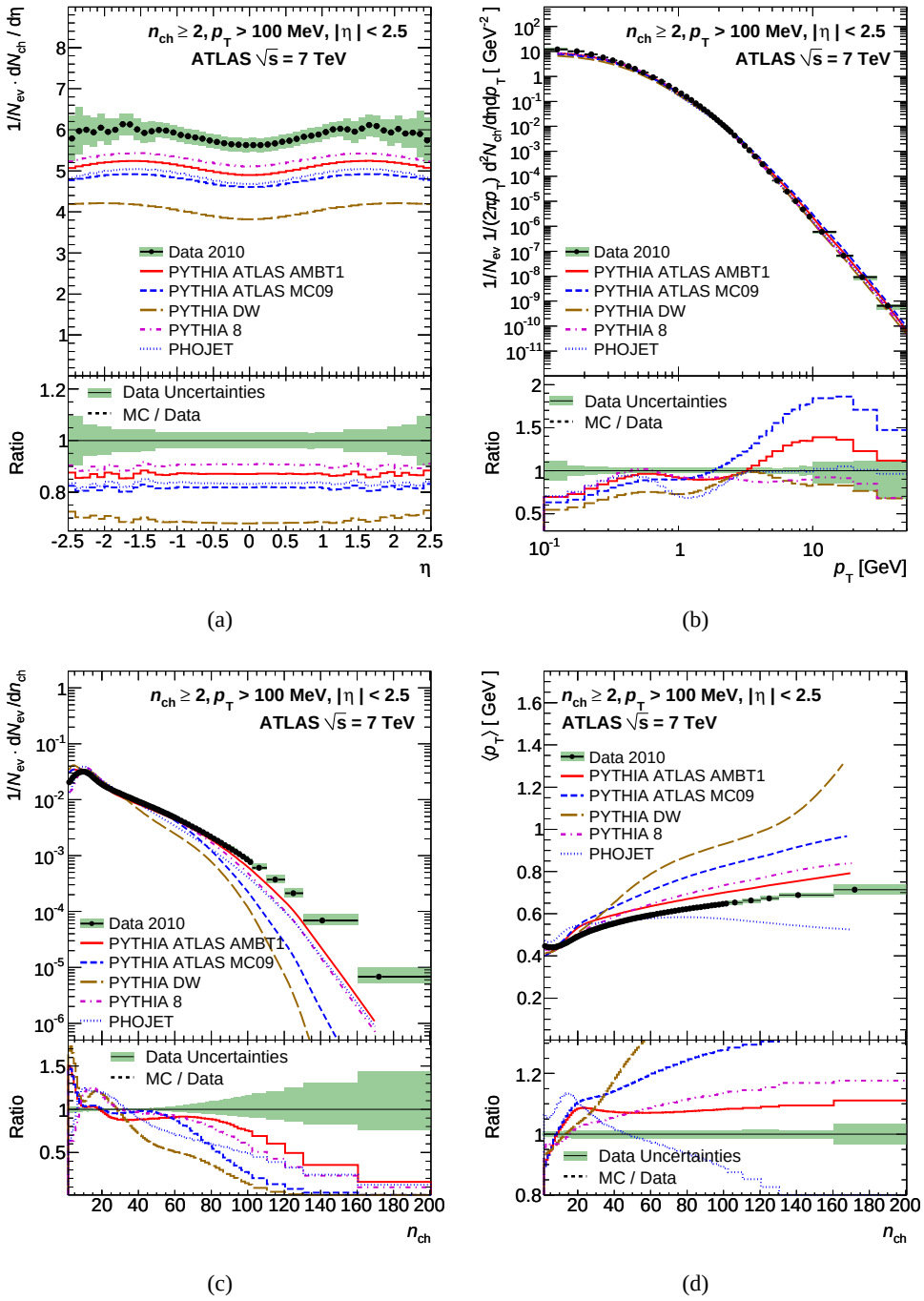

Figure 1: Charged-particle multiplicities as a function of (a) the pseudorapidity and (b) transverse momentum, (c) the charged-particle multiplicity distribution and (d) the average transverse momentum as a function of the number of charged particles . The plots are shown for events with $n_{\mathrm{ch}} \geq 2$, $p_{\mathrm{T}} > 100$ MeV at $\sqrt{s} = 7$ TeV. The dots represent the data and the curves the predictions from different MC models. The vertical bars represent the statistical uncertainties, while the shaded areas show statistical and systematic uncertainties added in quadrature. The bottom inserts show the ratio of the MC over the data. The values of the ratio histograms refer to the bin centroids.

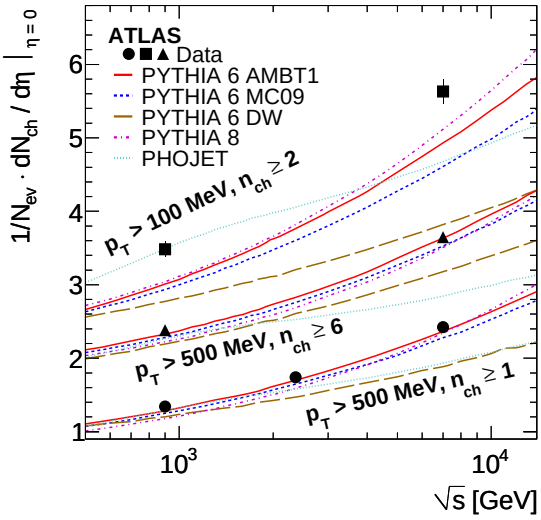

Figure 2: The average charged-particle multiplicity per unit of rapidity for $\eta = 0$ as a function of the centre-of-mass energy. The results with $n_{\mathrm{ch}} \geq 2$ within the kinematic range $p_{\mathrm{T}} > 100$ MeV and $|\eta| < 2.5$ are shown alongside the results with $n_{\mathrm{ch}} \geq 1$ and $n_{\mathrm{ch}} \geq 6$ within the kinematic range $p_{\mathrm{T}} > 500$ MeV and $|\eta| < 2.5$ at 0.9, 2.36 and 7 TeV. The data are compared to various particle level MC predictions. The vertical error bars on the data represent the total uncertainty.